H2O2 -Induced Persistent Luminescence Signal Enhancement Applied to Biosensing

Jianhua Liu, Bruno Viana, Nathalie Mignet, Daniel Scherman, Yingshuai Liu, Cyrille Richard

Nanoelectronics and Its New Materials – A NEW ERA OF NANOSCIENCE

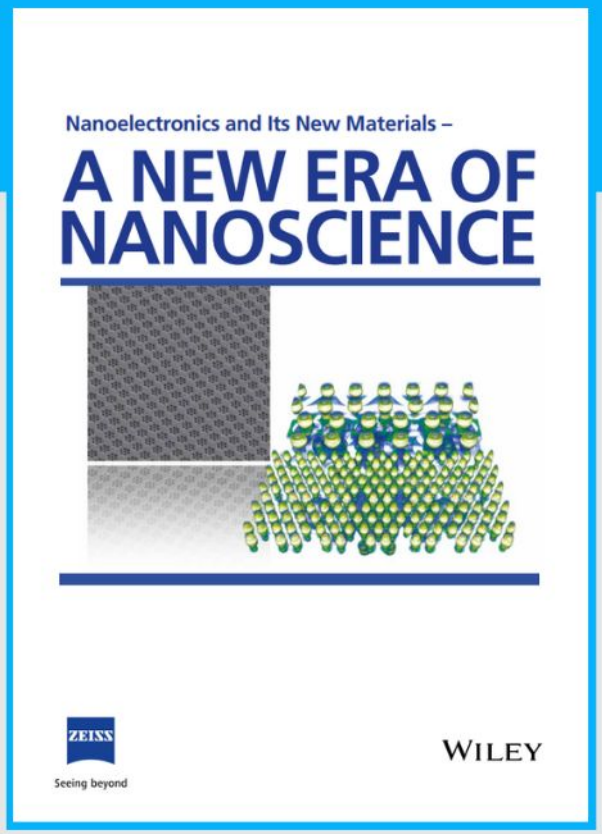

Discover the recent advances in electronics research and fundamental nanoscience.

Nanotechnology has become the driving force behind breakthroughs in engineering, materials science, physics, chemistry, and biological sciences. In this compendium, we delve into a wide range of novel applications that highlight recent advances in electronics research and fundamental nanoscience. From surface analysis and defect detection to tailored optical functionality and transparent nanowire electrodes, this eBook covers key topics that will revolutionize the future of electronics.

To get your hands on this valuable resource and unleash the power of nanotechnology, simply download the eBook now. Stay ahead of the curve and embrace the future of electronics with nanoscience as your guide.

ZEISS

Seeing beyond

WILEY

RESEARCH ARTICLE

NANO · MICRO small
www.small-journal.com

H_2O_2-Induced Persistent Luminescence Signal Enhancement Applied to Biosensing

Jianhua Liu, Bruno Viana, Nathalie Mignet, Daniel Scherman, Yingshuai Liu, and Cyrille Richard**

This work is dedicated to Prof. Daniel Scherman on the occasion of his 70th birthday

Persistent luminescence nanoparticles (PLNPs) are innovative materials able to emit light for a long time after the end of their excitation. Thanks to this property, their detection can be separated in time from the excitation, making it possible to obtain images with a high signal-to-noise ratio. This optical property can be of particular interest for the development of in vitro biosensors. Here, we report the unexpected effect of hydrogen peroxide (H_2O_2) on the signal intensity of $ZnGa_2O_4:Cr^{3+}$ (ZGO) nanoparticles. In the presence of H_2O_2, the signal intensity of ZGO can be amplified. This signal amplification can be used to detect and quantify H_2O_2 in various media, using non-functionalized ZGO nanoparticles. This small molecule can be produced by several oxidases when they react with their substrate. Indeed, the quantification of glucose, lactic acid, and uric acid is possible. The limit of detection could be lowered by modifying the nanoparticles synthesis route. These optimized nanoparticles can also be used as new biosensor to detect larger molecules such as antigen, using the appropriate antibody. This unique property, i.e., persistent luminescence signal enhancement induced by H_2O_2, represents a new way to detect biomolecules which could lead to a very large number of bioassay applications.

1. Introduction

Persistent luminescence is the property of some materials that are able to store the excitation energy from ultraviolet (UV), visible light to X-rays into traps or crystal defects referring either to dopants introduced during the synthesis or to irregular arrangement of the atoms in the crystal, such as oxygen vacancies, antisites, or interstitials.[1] Upon excitation, charge carriers (electrons and holes) are generated and can be trapped by these defects. When the excitation is stopped, and under thermal or optical activation, these trapped charges can leave the defects and recombine to emit light.[2] The emission signal can persist for minutes, hours, or even days depending on the composition and structure of the material. Since the first persistent luminescence phosphors (PLPs) discovered by Matsuzawa in 1996, made of strontium aluminate doped with europium

J. Liu[+], N. Mignet, D. Scherman, Y. Liu, C. Richard
Université Paris Cité
CNRS
INSERM
UTCBS
Unité de Technologies Chimiques et Biologiques pour la Santé
75006 Paris, France
E-mail: ysliu@swu.edu.cn; cyrille.richard@u-paris.fr

The ORCID identification number(s) for the author(s) of this article can be found under https://doi.org/10.1002/smll.202303509

[+]Present address: State Key Laboratory of Chemistry and Utilization of Carbon Based Energy Resources, College of Chemistry, Xinjiang University, 830017 Urumqi, China

B. Viana
Université PSL
CNRS IRCP
Chimie ParisTech
75005 Paris, France

Y. Liu
Key Laboratory of Luminescence Analysis and Molecular Sensing (Southwest University)
Ministry of Education
School of Materials and Energy
Southwest University
Chongqing 400715, China

DOI: 10.1002/smll.202303509

and dysprosium ($SrAl_2O_4$:Eu^{2+}, Dy^{3+}),[3] several PLPs with various matrix and dopants have been developed.[4–9] Several bulk PLPs, with sizes of few micrometers, emitting in the visible spectrum are now commercialized as night-vision materials for applications in security signs, traffic signs, dials, luminous paints, owing to their sufficiently strong and long persistent luminescence (>10 h) after excitation by sunlight or ambient light.[10] This property can also be obtained within nanoparticles. A couple of years ago, our group first demonstrated that persistent luminescence nanoparticles (PLNPs) made of a silicate matrix ($Ca_{0.2}Zn_{0.9}Mg_{0.9}Si_2O_6$) doped with Eu^{2+}, Dy^{3+}, and Mn^{2+} could emit persistent deep-red light at 700 nm and be used in vivo as new optical imaging agents.[11–13] In vivo imaging using persistent luminescence nanoprobes offers significant advantages for bioimaging compared to conventional fluorescent probes. Thanks to their long-lasting luminescence, the detection can be separated in time from the excitation, and the removal of the excitation during the signal acquisition is a solution to eliminate the background interference from tissue autofluorescence, thus providing images with high signal-to-noise ratio.[14] The original persistent nanophosphor was only excitable before injection with UV light, allowing performing imaging during 1 to 2 h after the injection. Following this pioneer work, others nanoprobes have been developed with improved performances, among which Cr^{3+} doped PLNPs, for which the persistent luminescence can be activated in situ, through the animal body, allowing performing imaging without any time limit.[15–18] It has been reported that such nanoprobes are not toxic to the animal[19–21] and they have been applied into various bioapplications,[22] for imaging and also for therapy.[23,24]Review papers and books on that topic have been recently published.[25–28]

This unique property of persistent emission is no longer only used in vivo but also in vitro for the development of new biosensors. In vitro optical detection is highly used in fundamental research and in clinic. Optical bioanalysis is one of the most common methods in analytical science, exhibiting many advantages such as visualization and fast measurement using simple and cheap operations. However, challenges remain for the sensitive analysis of complex samples, since interferences, either due to the presence of others (bio)molecules or to components used for the measurement (medium, tubes, plates) can generate autofluorescence under constant illumination and interfere with the signal to be measured. Consequently, the signal-to-noise ratio decreases, leading to a poor sensitivity. Therefore, it is of critical significance to find a way to eliminate the background interfering signal in order to improve the sensitivity for the analysis of samples, in particular when low concentration of analyte is present, notably for early diagnosis.[29,30] For this reason, PLNPs have been recently evaluated in vitro, allowing the detection of proteins such as α-fetoprotein and prostate specific antigen (PSA), small molecules such as ascorbic acid, dopamine, and also for cell apoptosis.[31–33] In these different cases, the detection is realized either through a turn-on (or turn-off) process or a resonance energy transfer (fluorescence resonance energy transfer, FRET or luminescence resonance energy transfer, LRET) between functionalized PLNPs and the analyte to be assayed or by the direct measurement of the signal emitted by the nanoparticles (NPs), which in all cases requires functionalized PLNPs.[34]

Herein, we report a different and novel strategy for the in vitro detection of biomolecules, based on the discovery that the signal intensity emitted by PLNPs made of $ZnGa_2O_4$:Cr^{3+} (ZGO) can be significantly enhanced by hydrogen peroxide (H_2O_2) in a dose-dependent manner. Although nanoparticles with optical properties are of great importance for biomedical applications, their quantum yield is always lower than the corresponding bulk materials. Traditionally, the most prevalent ways to enhance the signal intensity of persistent luminescence signal is either to prepare them at higher calcination temperature,[35,36] or to modify their composition by adding codopants,[37] to change the synthesis protocol[38] or to coat the surface with a silica shell.[39] All these cases involve new syntheses, which is costly and time consuming. Here, we report that enhancement of the persistent luminescence signal can be obtained by an easier, cheaper, and much faster way, without changing the composition of ZGO, simply by using already prepared ZGO NPs and by adding H_2O_2. Such a signal enhancement has never been reported before on materials with persistent luminescence, either in bulk or at the nanoscale.

H_2O_2 is the most common representative and stable reactive oxygen species (ROS) in living organisms.[40] H_2O_2 is a crucial biomarker in monitoring various diseases including diabetes, cancer, Parkinson's, cardiovascular, Alzheimer's, and neurodegenerative disorders.[41,42] Moreover, H_2O_2 quantification is also very important in vitro in enzyme-linked immunosorbent assays (ELISA) that generate or consume H_2O_2, which thus represents a potential intermediary biomolecule allowing the detection of disease-specific protein biomarkers, but also to evaluate the activity of the enzyme.[43] Hence, H_2O_2 is of high importance in diagnosis, and sensors of H_2O_2 are of broad interest in research and in clinical biochemical assays.[44]

2. Results and Discussion

2.1. Enhancement of Persistent Luminescence Signal Intensity of ZGO in the Presence of H_2O_2

The PLNPs used in the present study have been previously developed in our laboratory for in vivo imaging.[15] Briefly Zn^{2+}, Ga^{3+}, and Cr^{3+} nitrates are precipitated with ammonia, heated at 120 °C for 24 h, and calcinated at 750 °C for 5 h. The resulting powder is then crushed and stirred into HCl 50 mM for 16 h and centrifuged to extract 80 nm nanoparticles (Figure S1, Supporting Information). It is known that when a suspension of these NPs is excited by UV, after stopping the excitation, photons are emitted for several minutes, as seen in **Figure 1**a,i: this is the persistent luminescence property. Unexpectedly, we have discovered that when the same suspension is mixed with H_2O_2 and excited with UV, an increase of the signal intensity is observed (Figure 1a,ii). Figure 1b shows the effect of various concentrations of H_2O_2 on the signal intensity. As can be seen, the persistent luminescence decay, which represents the number of photons emitted over time, is affected by the amount of H_2O_2 added, the decay with the highest intensity being obtained when using the highest concentration of H_2O_2. When looking at the enhancement ratio, which corresponds to the value of the intensity of luminescence (counts) in the presence of H_2O_2 (L) divided by the value of the intensity of luminescence without H_2O_2 (L_0), this ratio increases when increasing the H_2O_2 concentration. An enhancement of luminescence

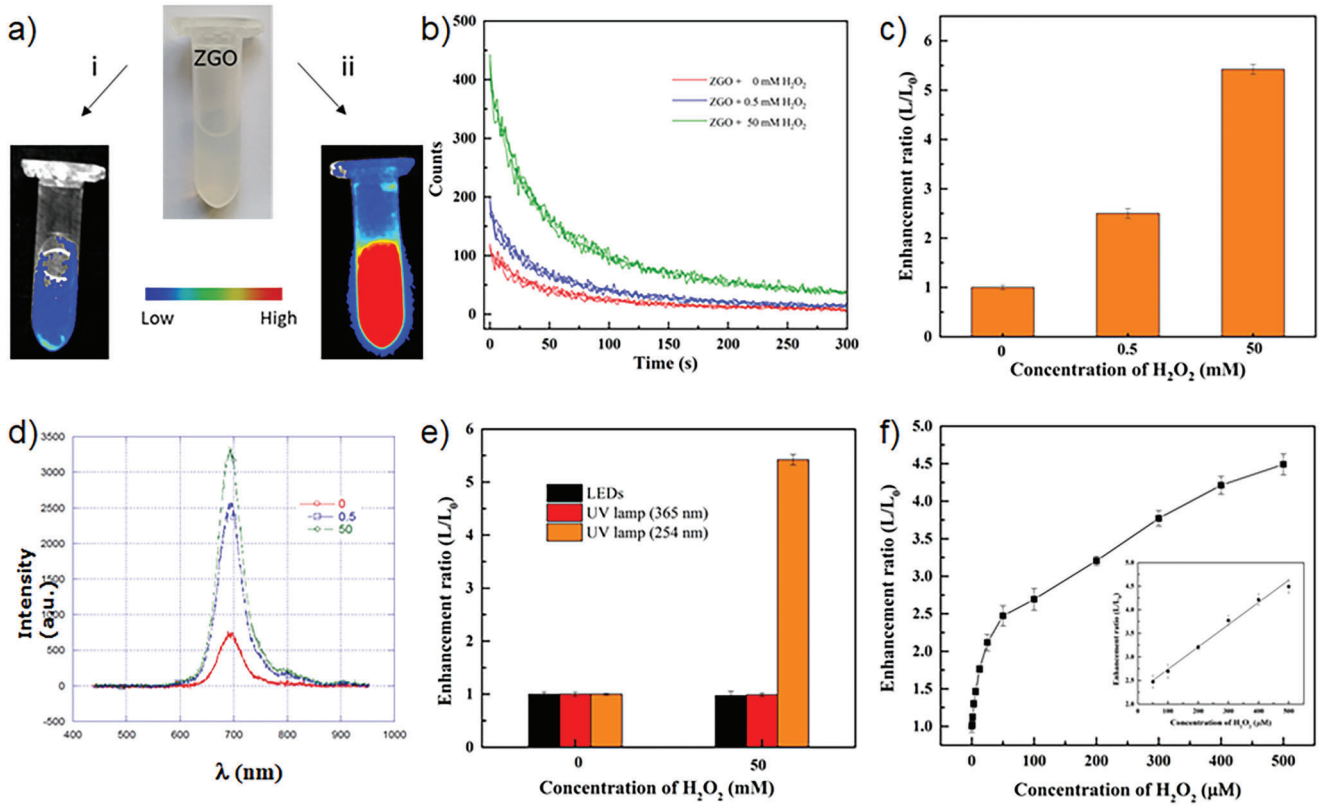

Figure 1. Effect of H_2O_2 on the persistent luminescence signal of ZGO. a) Excitation of a suspension of ZGO by UV i) without H_2O_2 or ii) in presence of H_2O_2. b) Persistent luminescence decay of ZGO with increasing amount of H_2O_2 (experiments realized in triplicate, $n = 3$). c) Enhancement ratio of ZGO in presence of increasing amount of H_2O_2 (0, 0.5, and 50 mM). d) Emission spectrum of ZGO with increasing amount of H_2O_2. e) Effect of irradiation source on the signal enhancement. f) Enhancement ratio applied to the dosage of H_2O_2. In the inset, linear relationship between the enhancement ratio and the concentration of H_2O_2. All acquisitions are carried out for 5 min after the excitation is stopped and experiments are done in triplicate.

of ≈5 is obtained with 50 mM H_2O_2 (Figure 1c). All acquisitions are carried out for 5 min after the excitation is stopped using the bioluminescence mode of a highly sensitive intensified CCD (ICCD) camera. It is worth noting that the amount of H_2O_2 added does not affect the emission peak, which is always centered at 698 nm.[45] This emission band is assigned to $^2E \rightarrow {}^4A_2$ transition of Cr^{3+} ions and its intensity increases with the increase of H_2O_2 (Figure 1d). When looking at the photoluminescence signal, we have also observed that this one is also amplified in the presence of H_2O_2 (Figure S2, Supporting Information).

It has already been reported that H_2O_2 can increase the signal intensity of molecular Eu^{3+} complexes[46] or Ag_2S quantum dots,[47] but on the other hand, it has also been reported that H_2O_2 can decrease (quench) the signal intensity of gold nanodots,[48] $NaYF_4$:Yb^{3+}/Er^{3+} upconversion nanoparticles,[49] Ce^{3+} doped vanadate,[50] Eu^{3+}-doped gadolinium or yttrium orthovanadate nanocrystals[51,52] and CaS:Ln^{3+} NPs,[53] and in most cases, this molecule has no influence on luminescence. It was therefore impossible to predict the effect of H_2O_2 on the signal of ZGO NPs, especially as H_2O_2 has never been previously reported to have an effect on materials with persistent luminescence, either in bulk or at the nanoscale. To propose an explanation to this phenomenon, two experiments have been performed. It has already been reported that the luminescence signal of some nanophosphors can be enhanced as a result of their aggregation. Indeed, Li et al. have shown that the luminescence of $La_{0.60}PO_4$:$Ce_{0.26}Tb_{0.14}$ nanoparticles can be increased by a factor 4 when these nanophosphors are aggregated.[54] To see if aggregation was responsible of the luminescence enhancement observed in our experiments, the hydrodynamic diameter of the ZGO nanoparticles dispersed in PBS was measured in the presence or in absence of H_2O_2 and with or without UV excitation (Figure S3, Supporting Information). As could be seen, the ZGO nanoparticles are stable in PBS whatever the conditions tested, so the signal enhancement cannot be explained by an aggregation effect. In the second experiment, it is known that H_2O_2 can decompose to different ROS, among which ·OH, under UV excitation.[55] We wondered whether such species could be involved in the signal enhancement, through electrons injection in the conduction band. For this purpose, we carried out experiments with an ·OH scavenger using dimethylsulfoxide (DMSO). Following, increasing amounts of DMSO have been added to the ZGO suspension mixed with 50 mM H_2O_2. As can be seen in Figure S4a in the Supporting Information, the addition of increasing percentage of DMSO (up to 50%) produces a decrease of the enhancement, suggesting that ·OH might be involved in the luminescence signal enhancement. We checked if DMSO could affect the luminescence of ZGO. We observed that

50% DMSO (without H_2O_2) does not affect the luminescence of ZGO (Figure S4b, Supporting Information), and when the experiment is done with H_2O_2 in pure DMSO, the signal is no longer enhanced (Figure S4c, Supporting Information), indicating that ROS generation (·OH) could be involved in the signal enhancement.

We have shown that this phenomenon can exist in different aqueous solutions, with the best enhancement obtained at pH 7.4 in PBS (Figure S5, Supporting Information). We have evaluated the effect of several parameters such as the irradiation time, the concentration of NPs, the temperature, the incubation time, the irradiation source, and the irradiation procedure. We first varied the irradiation time, from 10 s to 2 min and observed that the best enhancement was obtained with 40 s excitation time (Figure S6, Supporting Information). The concentration of ZGO was varied from 0.01 to 0.4 mg mL^{-1}. The best enhancement was obtained with a concentration of ZGO at 0.025 mg mL^{-1}, a concentration of H_2O_2 of 0.5 mM, and 40 s of UV excitation (Figure S7, Supporting Information). Since the persistent luminescence signal of ZGO is thermally stimulated, we checked the effect of the temperature on this phenomenon. Room temperature, 4 and 37 °C were investigated and we found that the temperature did not impact the signal enhancement in presence of 50 mM of H_2O_2 (Figure S8, Supporting Information). We have also evaluated the effect of incubation time and the experimental order in which H_2O_2 is introduced and irradiation is realized. The incubation time has no effect on the signal enhancement (Figure S9, Supporting Information), however if the irradiation of the NPs is done before mixing with H_2O_2, or if the excitation of ZGO and H_2O_2 is done separately before mixing, no enhancement occurs (Figure S10, Supporting Information). This phenomenon of signal enhancement is reversible and the removal of H_2O_2 from the medium allows recovering the initial signal level (Figure S11, Supporting Information). Finally, we have shown that the irradiation source has an important impact on the result, since among the three excitation sources tested (254 nm, 365 nm, and visible light emitting diode (LED)), only the 254 nm excitation allows getting the enhancement (Figure 1e). Finally, we have shown that with such parameters, we could apply this phenomenon for the dosage of H_2O_2. Figure 1f shows the enhancement ratio when increasing the concentration of H_2O_2 from 0 to 500 µM. A good linear relationship is obtained between 50 and 500 µM (Figure 1f, inset) and can be fitted as a linear function as $L/L_0 = 0.00472 \times C\ (\mu M) + 2.26642$ ($R^2 = 0.99$), allowing to determine the limit of detection (LOD) of H_2O_2 which is equal to 49.4 µM. The LOD was based on three times the standard deviation rule (LOD = 3 SD/S).[56]

It is the first time that an H_2O_2 assay based on persistent luminescence signal enhancement is reported. The following sections will enlarge the application of this phenomenon to the dosage of others small and also larger molecules.

2.2. In Vitro Application of Persistent Luminescence Signal Enhancement for the Dosage of Glucose, Uric Acid, and Lactic Acid

As mentioned in the Introduction, some enzymes are capable of producing H_2O_2 through reaction with their substrate.[57] As a proof of concept we chose glucose oxidase (GOD) to see if the in situ production of H_2O_2 could enhance the signal intensity of ZGO (**Figure 2**a). Glucose oxidase catalyzes the oxidation of glucose in the presence of oxygen to generate H_2O_2. The amount of H_2O_2 produced is directly proportional to the amount of glucose. Therefore, the enhancement of ZGO signal intensity in presence of GOD could directly allow to detect and quantity glucose.

For this purpose, GOD was incubated with glucose and ZGO in a microplate at 37 °C. After incubation, the plate was excited with a UV light and observed with an ICCD camera. As can be seen in Figure 2b, a significant increase of the luminescence signal is observed when ZGO, glucose, and GOD are together in the same well, in comparison to control experiments containing either only ZGO, ZGO with GOD, or ZGO with glucose, for which no enhancement occurs. As before, the persistent luminescence production is much higher when H_2O_2 is produced (i.e., when ZGO, glucose, and GOD are all together), compared to the control condition with only ZGO (Figure S12, Supporting Information). The influence of several parameters has also been tested, such as the incubation time and the GOD concentration. As can be seen in Figure S13 in the Supporting Information, the enhancement increases with the incubation time (time during which all three components are present together) and reaches a plateau after 1 h. As can be seen in Figure S14 in the Supporting Information, the luminescence signal increase with increasing the amount of GOD from 0 to 1 U mL^{-1} and then reaches a plateau. Then 1 U mL^{-1} was used for the further experiments. To assess if this procedure can be applied for the dosage of glucose, increasing amounts of glucose (from 0 to 250 µM) were incubated with GOD for 1 h. As can be seen in Figure 2c the enhancement increases with the amount of glucose. In the inset, a linear relationship is obtained when the concentration of glucose is between 62.5 and 250 µM which can be fitted as a linear function as $L/L_0 = 0.01113 \times C\ (\mu M) + 2.03443$ ($R^2 = 0.98$), allowing to determine the LOD of glucose, which is equal to 35.8 µM. To ensure that the luminescence enhancement is selective to glucose, the same experiment was repeated using other saccharides such as sucrose, maltose, fructose, galactose, mannose, xylose, and lactose, which are not substrates of GOD. As can be seen in Figure 2d, there is no signal enhancement when using saccharides other than glucose, demonstrating that ZGO based glucose sensor possesses high selectivity toward this molecule. We have shown that in addition of using this process for the dosage of glucose, it can also be used to check the activity of the enzyme. As can be seen in Figure S15 in the Supporting Information, the activity of the enzyme is dependent on the storage condition. When stored at −20 or 25 °C the enzyme keeps its activity, since the enhancement occurs; however, when heated at 90 °C it loses its activity and no enhancement occurs in the presence of glucose.

Glucose oxidase is not the only enzyme able to produce H_2O_2 by reaction with its substrate. In order to determine if this procedure can be generalized to assay other biomolecules, experiments have been also realized with other enzymes able to produce H_2O_2. For this purpose, experiments using uric acid and lactic acid have been performed using the same protocol, the only difference being the enzyme used, uricase or lactic oxidase instead of GOD. As can be seen in **Figure 3**a,b and Figure 3c,d, uric acid and lactic acid can be detected using the enhancement signal of ZGO using lactic oxidase or

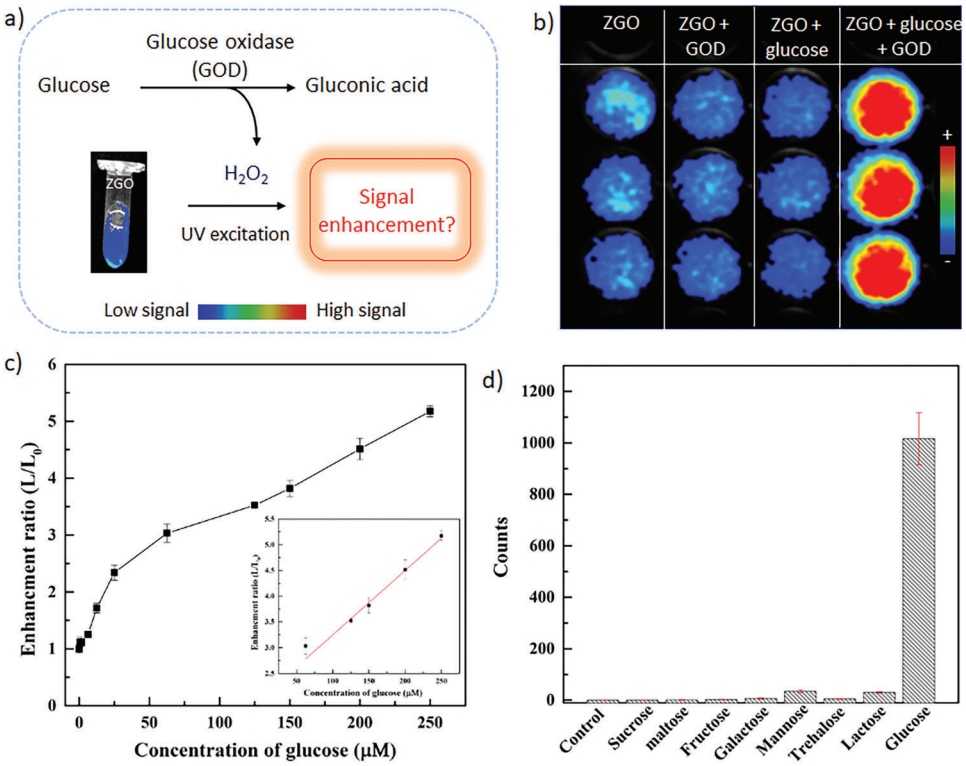

Figure 2. a) Principle of glucose detection based on H_2O_2 induced signal enhancement. b) Influence of operating conditions on the signal enhancement. c) Linearity area for glucose detection. d) Specificity of the technique for glucose detection. Experiments done in triplicate ($n = 3$).

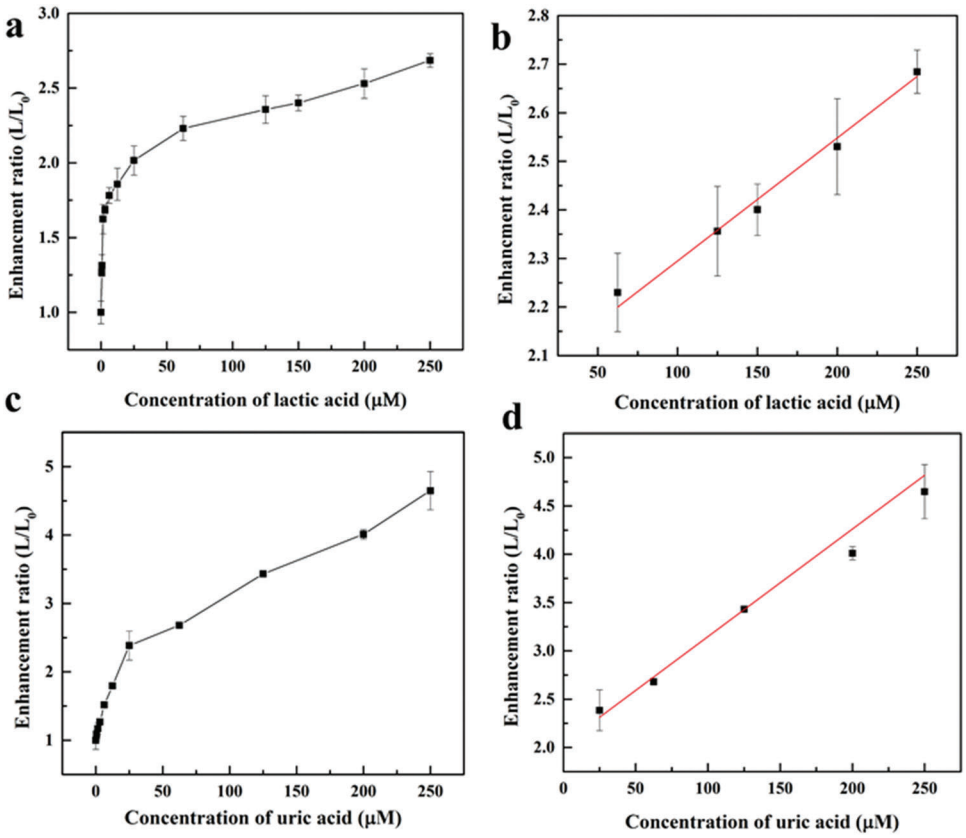

Figure 3. Application of signal enhancement for the dosage of a,b) lactic acid and c,d) uric acid. Experiments done in triplicate ($n = 3$).

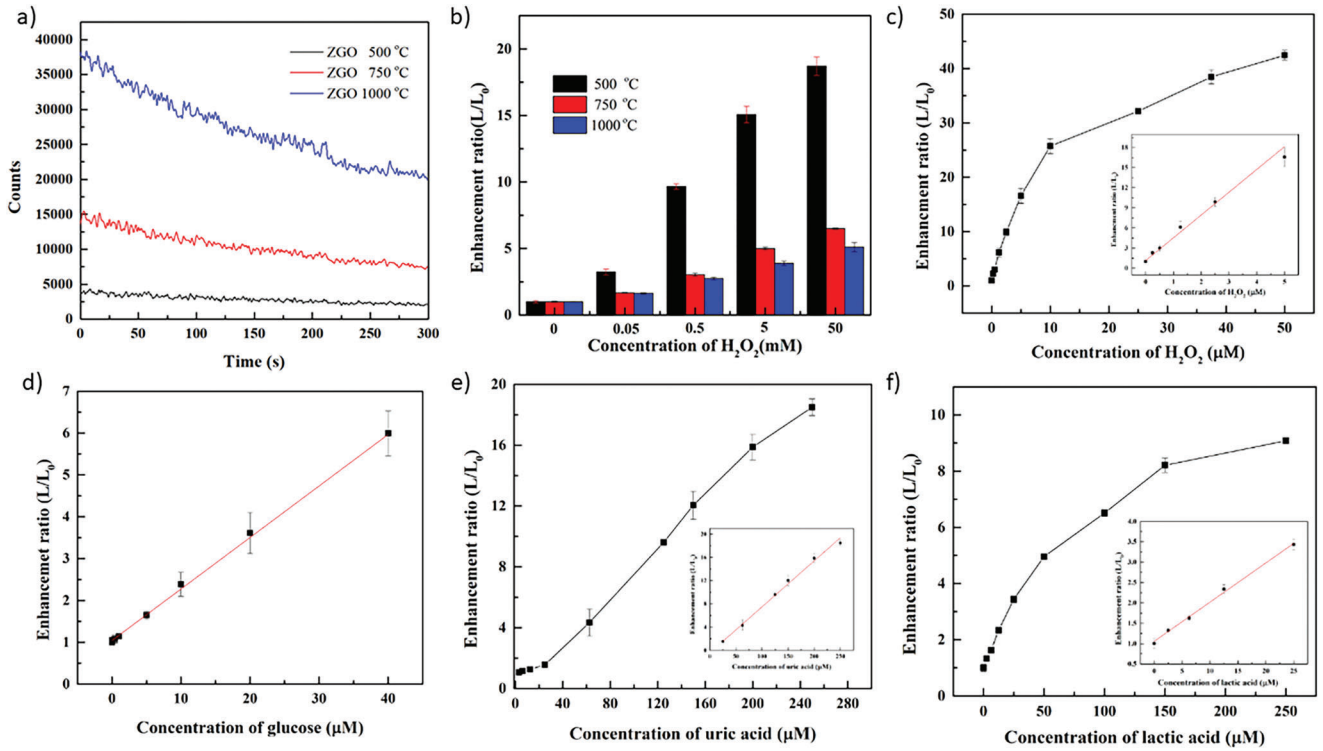

Figure 4. Improvement of signal enhancement. a) Effect of calcination temperature on the persistent luminescence signal. b) Effect of calcination temperature on persistent luminescence signal enhancement in presence of H_2O_2. c) Application to H_2O_2 detection. d–f) Application to glucose, uric acid, and lactic acid assay. The data presented in (c–f) were obtained using ZGO500 NPs. Experiments done in triplicate ($n = 3$).

uricase. A good linear relationship was obtained (Figure 3b) between the enhancement ratio and the concentration of lactic acid from 62.5 to 250 μM which can be fitted as a linear function as $L/L_0 = 0.00253 \times C\ (\mu M) + 2.04165$ ($R^2 = 0.99$), the LOD of lactic acid based on this method being 35.3 μM. For uric acid, a good linear relationship was also obtained (Figure 3d) between the enhancement ratio and the concentration of uric acid from 25 to 250 μM which can be fitted as a linear function as $L/L_0 = 0.00253 \times C\ (\mu M) + 2.04165$ ($R^2 = 0.99$), and the LOD was 20.07 μM.

As for glucose, it is the first time that lactic acid and uric acid are detected and quantified using the signal enhancement of persistent luminescence nanoparticles. We have compared our data for the dosage of H_2O_2, glucose, lactic acid, and uric acid with several published ones. Most of the time, our method gives better LOD, but not always (see Tables S1–S4, Supporting Information). To improve these results, and to compete with the best reported methods, we have worked on a particular step of the preparation of our nanosensor.

2.3. Improvement of the Performance of ZGO NPs to Lower the LOD

As mentioned in the Introduction, the ZGO nanoparticles we have used in Sections 2.1 and 2.2 were initially prepared for in vivo imaging applications and calcinated at 750 °C. However, in order improve the detection of biomolecules by lowering the LOD, we decided to evaluate the impact of a particular step in the synthesis of the ZGO, the calcination temperature (last step of the synthesis, Figure S16, Supporting Information). To do this, we used the ZGO powder remaining after the hydrothermal treatment (step 3 in Figure S16, Supporting Information) and evaluated the effect of two others calcination temperature, a lower one, 500 °C and a higher one, 1000 °C. Comparison of intensity of persistent luminescence decay of ZGO prepared at these temperatures is reported in **Figure 4**a. As expected, the calcination temperature has an impact on the signal of the material and calcination at 500 °C produces ZGO with the lowest signal intensity whereas calcination at 1000 °C produces ZGO with the highest signal intensity.[58] Nanometer nanoparticles (80 nm, same size as before), prepared either at 500 °C, 750 °C, or at 1000 °C and dispersed into PBS were mixed with different concentrations of H_2O_2 (0.05, 0.5, 5, and 50 mM) and excited with UV. As can be seen in Figure 4b, the temperature at which the ZGO have been calcinated has a strong impact on the H_2O_2 induced enhancing effect. Indeed, the best enhancement being observed when the calcination is carried out at 500 °C, which corresponds to ZGO with the lowest signal intensity. Here again, the impact of the temperature calcination on the enhancement signal intensity of ZGO in presence of H_2O_2 was difficult to predict. This new sample (ZGO500) was used as above to assay the different biomolecules (H_2O_2, glucose, lactic acid and uric acid), in order to see its ability to lower the LOD. As shown above, we can see that the enhancement is linear with the concentration of H_2O_2 (Y (L/L_0) = 3.4C (μM) + 1.138 ($R^2 = 0.99$), allowing to determine

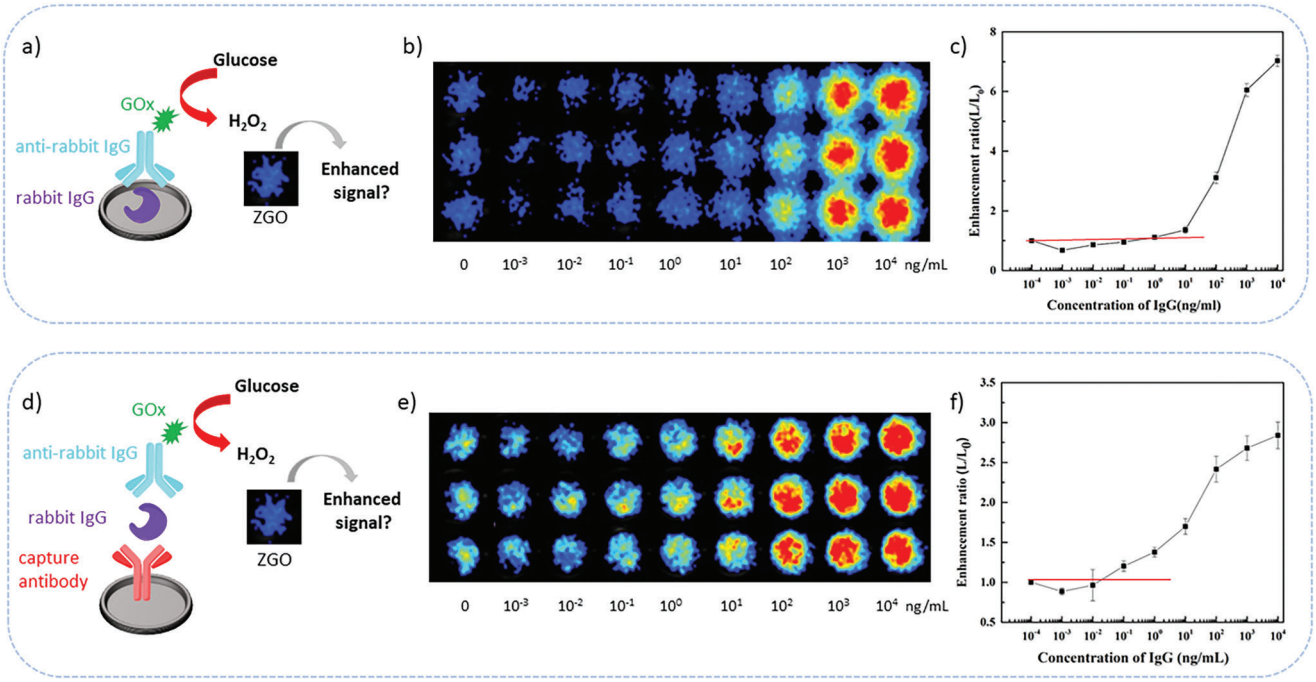

Figure 5. a) Principle of antigen detection based on signal enhancement using direct ELISA experiment. b) Persistent luminescence signal versus [IgG]. Experiments done in triplicate ($n = 3$). c) Signal enhancement versus [IgG]. d) Principle of antigen detection based on signal enhancement using a sandwich ELISA protocol. e) Persistent luminescence signal versus [IgG]. Experiments done in triplicate ($n = 3$). f) Signal enhancement versus [IgG]. Experiments done in triplicate ($n = 3$).

the LOD of H_2O_2 which is dramatically decreased to 0.13 µM (Figure 4c). As compared to previous experiment using ZGO calcinated at 750 °C (Section 2.1), we have been able to lower the LOD by a factor ≈250 (>2 log). The detection performance based on the signal enhancement is now superior to those of many previously reported techniques (Table S1, Supporting Information).

Encouraged by this result, we wondered whether we could also lower the LOD of glucose, uric acid, and lactic acid. Similar experiments as those presented in Section 2.2 were realized, the only modifications being that the measurements were done now using ZGO500 NPs.

We first repeated the dosage of glucose. As can be seen in Figure 4d, the enhancement is still linear with the concentration of glucose, allowing to determine the LOD of glucose which is 0.21 µM. This value is now lower than the ones reported in Table S2 in the Supporting Information. Compared to previous experiment (Section 2.2) we were able to lower the LOD by a factor 170 (>2 log).

When we did the same using uric acid (Figure 4e), we were able to get an LOD = 2.8 µM, a value being almost ten times more performant than with 750 °C ZGO NPs. For lactic acid an LOD = 0.99 µM was obtained, which is 36 times lower than before (Figure 4f) and among the best ones when compared with published data (Tables S3 and S4, Supporting Information).

2.4. Application to Antigen Detection

To broaden the scope of application of this phenomenon, as a last example, we applied this concept in a little more complicated procedure in order to see if larger molecules, such as antigen, can be detected and quantify. For this purpose, as a proof of concept, a direct ELISA-like protocol using rabbit IgG, as a model antigen was chosen (**Figure 5**a). Microplate wells were first incubated with increasing amounts of antigens, from 10^{-3} to 10^{4} ng mL^{-1}, and after washing steps, antirabbit IgG labeled with GOD was added. After incubation and washing, a fix amount of glucose and ZGO was added, as it was previously done in the former experiment (Figure 2a). As can be seen in Figure 5b, a difference in the signal intensity can be detected between the different conditions, the highest amount of IgG deposited on the plate giving higher signal. Finally, when reporting the enhancement value versus [IgG], a nonlinear relationship can be obtained, allowing to determine the lowest concentration of IgG we can detect using this method, which corresponds to 1 ng mL^{-1}. This was already pretty good, but by slightly modifying the protocol, using a sandwich ELISA-like protocol (Figure 5d), we were able to not only confirm the feasibility of using persistent luminescence signal enhancement to detect and assay the antigen, but in addition to lower the LOD to 0.1 ng mL^{-1} (Figure 5e,f). When compared with other published works, our method finally competed with the best published methods (Table S5, Supporting Information).

3. Conclusion

We reported, for the first time, the unexpected effect of H_2O_2 on the luminescence signal of ZGO NPs. The aim of this work was to exploit the property of persistent luminescence as a solution to eliminate the background interference observed when using fluorescent biosensors and to take advantage of the

persistent luminescence signal enhancement as a solution to improve detection. We have shown that this enhancement effect can be applied to assay several biomolecules via enzymatic H_2O_2 production. By adjusting the calcination temperature of ZGO and starting from a material with low emission intensity, we were able to strongly enhance the emission signal, which allowed us to lower the LOD and compete with the most performant published methods. This is the first time that signal enhancement of PLNPs based on the presence of H_2O_2 has been applied to biosensing. This new method has several advantages: it is an easy strategy since no ZGO coating is needed, it is inexpensive since the ZGO synthesis uses cheap salts, the ZGO NPs are not light sensitive and can be stored at room temperature without any special attention (unlike most fluorescent dyes) and the amount of NPs needed for experiments is very small (≈5 µg).

Future work is planned to show that this phenomenon can be generalized and applied to the assay of other biomolecules. The influence of other excitation sources[59,60] will be evaluated and deeper efforts will be made to better understand the signal enhancement phenomenon to further improve the efficiency of the sensor. This unique property, i.e., persistent luminescence signal enhancement induced by H_2O_2, constitutes a completely new way of detecting biomolecules.

4. Experimental Section

Preparation of ZGO Nanoparticles: The ZGO nanoparticles were prepared according to previous work.[15] In brief, 8.94 mmol of gallium oxide were dissolved in 10 mL concentrated HNO_3 (35%), then the mixture sample was transferred to Teflon-lined stainless-steel autoclave and heated at 150 °C overnight. After that step, 0.04 mmol of $Cr(NO_3)_3.9H_2O$ and 8.97 mmol of $Zn(NO_3)_2.6H_2O$ were dissolved in 10 mL deionized water and the obtained solution was mixed with the previous solution of $Ga(NO_3)_3$ under stirring (step 1, Figure S16, Supporting Information). Then, ammonia solution was added drop by drop to adjust its pH value to 7.5 (step 2, Figure S16, Supporting Information). After that, the obtained solution was stirred for 3 h at room temperature before transferring to Teflon-lined stainless-steel autoclave and heated at 120 °C for 24 h (hydrothermal treatment, step 3, Figure S16, Supporting Information). Finally, the resulted product was washed with water and ethanol several times and then dried at 60 °C. The obtained white powder was sintered at 750 °C for 5 h (calcination step, step 4, Figure S16, Supporting Information).

In order to obtain nanosized ZGO, the powder was grinded for 15 min in the presence of HCl (5 mM) with a mortar and pestle, transferred into 50 mL HCl and the suspension was stirred overnight to recover 80 nm ZGO NPs after centrifugation.

For ZGO prepared at 500 and 1000 °C, the procedure was the same except the calcination temperature (step 4, Figure S16, Supporting Information) which is either realized at 500 or 1000 °C.

Detection of H_2O_2: All the detection experiments were carried out in 96-well plates. The signal was captured by photon-counting system for 5 min after UV excitation (wavelength is a 254 nm Hg lamp (6 W), intensity 2.2 (W/Sr) (1500 cd), irradiance 21 W m^{-2}, the exposure time is 40 s. For H_2O_2 detection, 50 µL of ZGO (concentration of ZGO750 is 0.05 mg mL^{-1} or concentration of ZGO500 is 0.1 mg mL^{-1}) in PBS and 50 µL of different concentration of H_2O_2 were added to each well of plate. After incubation for 5 min, the signal was captured by the photon-counting device after UV excitation and analyzed by M3 vision software.

Glucose, Uric Acid, and Lactic Acid Detection: Glucose detection was carried out as follow: in a microplate, 25 µL GOD, 50 µL ZGO (concentration of ZGO750 is 0.05 mg mL^{-1} or concentration of ZGO500 is 0.1 mg mL^{-1}) and 25 µL glucose at different concentrations were added into each well. After incubation for 1 h at 37 °C to produce H_2O_2, the signal enhancement was measured and analyzed as before.

For uric acid and lactic acid detection, the procedure was the same as for glucose detection, except that GOD was replaced by uricase or lactic oxidase, and glucose was replaced by uric acid or lactic acid.

ELISA-Like Experiments: *Direct ELISA*: In a typical procedure, 100 µL of different concentration of rabbit IgG (10^{-3}, 10^{-2}, 10^{-1}, 10^{0}, 10^{1}, 10^{2}, 10^{3}, and 10^{4} ng mL^{-1}, in 50 mM carbonate-bicarbonate (CBS) buffer, pH 9.6) were incubated overnight at 4 °C. After washing three times with phosphate buffered saline (PBS) with 0.05% Tween 20 (PBST, pH 7.4), 300 µL of bovine serum albumin (BSA) solution (1.0 mg mL^{-1}, in PBS) was used to block the excess sites of the wells and incubated at 37 °C for 60 min. After washing three times with PBST, 100 µL of goat antirabbit IgG labelled with GOD (200 times dilution, in PBS) were added into the plate and incubated at 37 °C for 60 min. After washing three times with PBST and two times with PBS, 50 µL of glucose (100 mM) and 50 µL of ZGO (0.1 mg mL^{-1}) were added into the well of the plate and incubated at 37 °C for 60 min. The signal was captured by the photon-counting device after 40 s UV excitation.

Sandwich ELISA: A 96-well plate was first coated with 100 µL of monoclonal anti-rabbit IgG (10 µg mL^{-1}, 50 mM CBS buffer, pH 9.6) and incubated overnight at 4 °C. After washing three times with PBST, 300 µL of BSA solution (1.0 mg mL^{-1}, in PBS) was used to block the excess sites of the wells and incubated at 37 °C for 60 min. After that step, 100 µL of different concentration of rabbit IgG (10^{-3}, 10^{-2}, 10^{-1}, 10^{0}, 10^{1}, 10^{2}, 10^{3}, and 10^{4} ng mL^{-1}, in PBS) were added into the plate and incubated at 37 °C for 60 min. After washing three times with PBST, 100 µL of goat anti-rabbit IgG labeled with GOD (200 times dilution, in PBS) were added into the plate and incubated at 37 °C for 60 min. After washing three times with PBST and two times with PBS, 50 µL of glucose (100 mM) and 50 µL of ZGO (0.1 mg mL^{-1}) were added into the well of the plate and incubated at 37 °C for 60 min. The signal was captured by the photon-counting device after UV excitation.

Supporting Information

Supporting Information is available from the Wiley Online Library or from the author.

Acknowledgements

The authors acknowledge Prof. D. Gourier from Chimie-ParisTech, IRCP for helpful discussions. J.H.L. thanks China Scholarship Council (CSC) for the PhD scholarship and Y.S.L. thanks CSC for the visiting scholar grant. The authors acknowledge the following grants for financial support: Natural Science Foundation Project of Chongqing, China (cstc2021jcyj-msxmX1081) and French Research Agency: Agence Nationale de la Recherche (ANR) PLEaSe project (ANR-22-CE09-0029-01).

Conflict of Interest

The authors declare no conflict of interest.

Data Availability Statement

The data that support the findings of this study are available from the corresponding author upon reasonable request.

Keywords

biosensors, diagnostic, H_2O_2, nanoparticles, persistent luminescence, signal enhancement

Received: April 26, 2023
Revised: June 23, 2023
Published online:

[1] J. Xu, S. Tanabe, *J. Lumin.* **2019**, *205*, 581.
[2] Y. Li, M. Gecevicius, J. R. Qiu, *Chem. Soc. Rev.* **2016**, *45*, 2090.
[3] T. Matsuzawa, Y. Aoki, N. Takeuchi, Y. Murayama, *J. Electrochem. Soc.* **1996**, *143*, 2670.
[4] B. Viana, S. K. Sharma, D. Gourier, T. Maldiney, E. Teston, D. Scherman, C. Richard, *J. Lumin.* **2016**, *170*, 887.
[5] S. K. Sharma, D. Gourier, E. Teston, D. Scherman, C. Richard, B. Viana, *Opt. Mater.* **2017**, *63*, 51.
[6] M. Pellerin, E. Glais, T. Lecuyer, J. Xu, J. Seguin, S. Tanabe, C. Chanéac, B. Viana, C. Richard, *J. Lumin.* **2018**, *202*, 83.
[7] J. Ueda, J. L. Leano Jr., C. Richard, K. Asami, S. Tanabe, R.-S. Liu, *J. Mater. Chem. C* **2019**, *7*, 1705.
[8] Z. Pan, V. Castaing, L. Yan, L. Zhang, C. Zhang, K. Shao, Y. Zheng, C. Duan, J. Liu, C. Richard, B. Viana, *J. Phys. Chem. C* **2020**, *124*, 8347.
[9] V. Castaing, L. Giordano, C. Richard, D. Gourier, M. Allix, B. Viana, *J. Phys. Chem. C* **2021**, *125*, 10110.
[10] https://www.nemoto.co.jp/nlm (accessed: january 2023).
[11] Q. le Masne de Chermont, C. Chanéac, J. Seguin, F. Pellé, S. Maîtrejean, J. P. Jolivet, D. Gourier, M. Bessodes, D. Scherman, *Proc. Natl. Acad. Sci. U. S. A.* **2007**, *104*, 9266.
[12] T. Maldiney, C. Richard, J. Seguin, N. Wattier, M. Bessodes, D. Scherman, *ACS Nano* **2011**, *5*, 854.
[13] T. Maldiney, M. U. Kaikkonen, J. Seguin, Q. le Masne de Chermont, M. Bessodes, K. J. Airenne, S. Ylä-Herttuala, D. Scherman, C. Richard, *Bioconjugate Chem.* **2012**, *23*, 472.
[14] T. Maldiney, A. Lecointre, B. Viana, A. Bessiere, M. Bessodes, D. Gourier, C. Richard, D. Scherman, *J. Am. Chem. Soc.* **2011**, *133*, 11810.
[15] T. Maldiney, A. Bessière, J. Seguin, E. Teston, S. K. Sharma, B. Viana, A. J. J. Bos, P. Dorenbos, M. Bessodes, D. Gourier, D. Scherman, C. Richard, *Nat. Mater.* **2014**, *13*, 418.
[16] Z. Li, Y. Zhang, X. Wu, L. Huang, D. Li, W. Fan, G. Han, *J. Am. Chem. Soc.* **2015**, *137*, 5304.
[17] E. Teston, S. Richard, T. Maldiney, N. Lièvre, G. Yangshu Wang, L. Motte, C. Richard, Y. Lalatonne, *Chem. - Eur. J.* **2015**, *21*, 7350.
[18] F. Liu, W. Yan, Y. J. Chuang, Z. Zhen, J. Xie, Z. Pan, *Sci. Rep.* **2013**, *3*, 1554.
[19] G. Ramírez-Garcíaa, S. Gutiérrez-Granados, M. A. Gallegos-Corona, L. Palma-Tirado, F. d'Orlyé, A. Varenne, N. Mignet, C. Richard, M. Martínez- Alfaro, *Int. J. Pharm.* **2017**, *532*, 686.
[20] Y. Jiang, Y. Li, C. Richard, D. Scherman, Y. Liu, *J. Mater. Chem. B* **2019**, *7*, 3796.
[21] T. Lécuyer, J. Seguin, A. Balfourier, M. Delagrange, P. Burckel, R. Lai-Kuen, V. Mignon, B. Ducos, M. Tharaud, B. Saubaméa, D. Scherman, N. Mignet, F. Gazeau, C. Richard, *Nanoscale* **2022**, *14*, 15760.
[22] L. Giordano, G. Cai, J. Seguin, J. Liu, C. Richard, L. C. V. Rodrigues, B. Viana, *Adv. Opt. Mater.* **2023**, *11*, 2201468.
[23] T. Maldiney, B. T. Doan, D. Alloyeau, M. Bessodes, D. Scherman, C. Richard, *Adv. Funct. Mater.* **2015**, *25*, 331.
[24] E. Teston, T. Maldiney, I. Marangon, J. Volatron, Y. Lalatonne, L. Motte, C. Boisson-Vidal, G. Autret, O. Clément, D. Scherman, F. Gazeau, C. Richard, *Small* **2018**, *14*, 1800020.
[25] T. Lécuyer, E. Teston, G. Ramirez-Garcia, T. Maldiney, B. Viana, J. Seguin, N. Mignet, D. Scherman, C. Richard, *Theranostics* **2016**, *6*, 2488.
[26] J. Liu, T. Lécuyer, J. Seguin, N. Mignet, D. Scherman, B. Viana, C. Richard, *Adv. Drug Delivery Rev.* **2019**, *138*, 193.
[27] B. Viana, C. Richard, V. Castaing, E. Glais, M. Pellerin, J. Liu, C. Chanéac, *Near Infrared-Emitting Nanoparticles for Biomedical Applications*, Springer Nature, Switzerland AG **2020**, https://doi.org/10.1007/978-3-030-32036-2_8.
[28] K. Huang, N. Le, J. S. Wang, L. Huang, L. Zeng, W. C. Xu, Z. Li, Y. Li, G. Han, *Adv. Mater.* **2022**, *34*, 2107962.
[29] S. K. Sun, H. F. Wang, X. P. Yan, *Acc. Chem. Res.* **2018**, *51*, 1131.
[30] X. Sun, L. Song, N. Liu, J. Shi, Y. Zhang, *ACS Appl. Nano Mater.* **2021**, *4*, 6497.
[31] N. Li, Y. Li, Y. Han, W. Pan, T. Zhang, B. Tang, *Anal. Chem.* **2014**, *86*, 3924.
[32] L. Zhang, J. Lei, J. Liu, F. Ma, H. Ju, *Biomaterials* **2015**, *67*, 323.
[33] B. Y. Wu, X. P. Yan, *Chem. Commun.* **2015**, *51*, 3903.
[34] A. S. Paterson, B. Raja, G. Garvey, A. Kolhatkar, A. E. Hagström, K. Kourentzi, T. R. Lee, R. C. Willson, *Anal. Chem.* **2014**, *86*, 9481.
[35] T. Lecuyer, E. Teston, T. Maldiney, D. Scherman, C. Richard, *SPIE Proc.* **2016**, *9722*, https://doi.org/10.1117/12.2207477.
[36] X. H. Lin, L. Song, S. Chen, X. F. Chen, J. J. Wei, J. Li, G. Huang, H. H. Yang, *ACS Appl. Mater. Interfaces* **2017**, *9*, 41181.
[37] Y. Zhao, J. Du, X. Wu, Y. Wang, D. Poelman, *J. Lumin.* **2020**, *220*, 117035.
[38] B. B. Srivastava, S. K. Gupta, Y. Mao, *CrystEngComm* **2020**, *22*, 2491.
[39] L. Fu, J. Wang, N. Chen, Q. Ma, D. Lu, Q. Yuan, *Chem. Commun.* **2020**, *56*, 6660.
[40] S. G. Rhee, *Science* **2006**, *312*, 1882.
[41] G. Y. Liou, P. Storz, *Free Radic. Res.* **2010**, *44*, 479.
[42] K. J. Barnham, C. L. Masters, A. I. Bush, *Nat. Rev. Drug Discovery* **2004**, *3*, 205.
[43] R. de la Rica, M. M. Stevens, *Nat. Nanotechnol.* **2012**, *7*, 821.
[44] V. Patel, P. Kruse, P. R. Selvaganapathy, *Biosensors* **2021**, *11*, 9.
[45] A. Bessière, S. K. Sharma, N. Basavaraju, K. R. Priolkar, L. Binet, B. Viana, A. J. J. Bos, T. Maldiney, C. Richard, D. Scherman, D. Gourier, *Chem. Mater.* **2014**, *26*, 1365.
[46] O. S. Wolfbeis, A. Dürkop, M. Wu, Z. Lin, *Angew. Chem., Int. Ed.* **2002**, *41*, 4495.
[47] X. Zhang, W. Wang, L. Su, X. Ge, J. Ye, C. Zhao, Y. He, H. Yang, J. Song, H. Duan, *Nano Lett.* **2021**, *21*, 2625.
[48] Y. C. Shiang, C. C. Huang, H. T. Chang, *Chem. Commun.* **2009**, *23*, 3437.
[49] J. Liu, L. Lu, A. Li, J. Tang, S. Wang, S. Xu, L. Wang, *Biosens. Bioelectron.* **2015**, *68*, 204.
[50] D. Casanova, C. Bouzigues, T. L. Nguyên, R. O. Ramodiharilafy, L. Bouzhir-Sima, T. Gacoin, J. P. Boilot, P. L. Tharaux, A. Alexandrou, *Nat. Nanotechnol.* **2009**, *4*, 581.
[51] V. Muhr, M. Buchner, T. Hirsch, D. J. Jovanovic, S. D. Dolic, M. D. Dramicanin, O. S. Wolfbeis, *Sens. Actuators, B* **2017**, *241*, 349.
[52] N. Duée, C. Ambard, F. Pereira, D. Portehault, B. Viana, K. Vallé, D. Autissier, C. Sanchez, *Chem. Mater.* **2015**, *27*, 5198.
[53] M. Zhang, W. Zheng, Y. Liu, P. Huang, Z. Gong, J. Wei, Y. Gao, S. Zhou, X. Li, X. Chen, *Angew. Chem., Int. Ed.* **2019**, *58*, 9556.
[54] L. Li, W. Jiang, H. Pan, X. Xu, Y. Tang, J. Ming, Z. Xu, R. Tang, *J. Phys. Chem. C* **2007**, *111*, 4111.
[55] M. A. Oturan, J. J. Aaron, *Crit. Rev. Environ. Sci. Technol.* **2014**, *44*, 2577.
[56] R. Zhang, S. He, C. Zhang, W. Chen, *J. Mater. Chem. B* **2015**, *3*, 4146.
[57] D. Bruen, C. Delaney, L. Florea, D. Diamond, *Sensors* **2017**, *17*, 1866.
[58] P. Huang, C. E. Cui, S. Wang, *Opt. Mater.* **2009**, *32*, 184.
[59] C. Richard, B. Viana, *Light: Sci. Appl.* **2022**, *11*, 123.
[60] K. Huang, X. Dou, Y. Zhang, X. Gao, J. Lin, J. Qu, Y. Li, P. Huang, G. Han, *Adv. Funct. Mater.* **2021**, *31*, 2009920.